Large Eddy Simulation of Flow through an Axisymmetric Sudden Expansion

June 2022

Byung-Hee Choi, N.K. Anand, Yassin A. Hassan, Piyush Sabharwall

Changing the World's Energy Future

INL
Idaho National Laboratory

Large Eddy Simulation of Flow through an Axisymmetric Sudden Expansion

Byung-Hee Choi, N.K. Anand, Yassin A. Hassan, Piyush Sabharwall

June 2022

Idaho National Laboratory
Idaho Falls, Idaho 83415

http://www.inl.gov

Large eddy simulation of flow through an axisymmetric sudden expansion

Byung-Hee Choi (최병희), N. K. Anand, Yassin A. Hassan, et al.

COLLECTIONS

F   This paper was selected as Featured

View Online   Export Citation   CrossMark

ARTICLES YOU MAY BE INTERESTED IN

Physics of Fluids

Special Topic: Paint and Coating Physics

Submit Today!

Large eddy simulation of flow through an axisymmetric sudden expansion Ⓕ

View Online   Export Citation   CrossMark

Byung-Hee Choi (최병희),[1,a)] ⓘD N. K. Anand,[1] Yassin A. Hassan,[2] and Piyush Sabharwall[3] ⓘD

AFFILIATIONS

[1]Department of Mechanical Engineering, Texas A&M University, College Station, Texas 77843, USA
[2]Department of Nuclear Engineering, Texas A&M University, College Station, Texas 77843, USA
[3]Idaho National Laboratory, Idaho Falls, Idaho 83415, USA

[a)]Author to whom correspondence should be addressed: bagbagwan@tamu.edu

ABSTRACT

This study aims at investigating the inlet flow conditions of flow through an axisymmetric sudden expansion with an expansion ratio of 2.0. A series of large eddy simulations with the WALE model were conducted for different inlet Reynolds numbers (Re) and turbulence intensities ($u_{rms}/\bar{U}_m$). The reattachment length, defined as the length measured downstream of the expansion where the flow direction is reversed adjacent to the wall (Lr), was measured for each case. For widely studied inlet turbulence intensity values (TI), the simulation results are in good agreement with the experimental and numerical results reported in the literature. Parametric studies revealed that turbulence intensity affects the critical Reynolds number, marking the transition between the laminar and transition regions and the reattachment length. The critical Reynolds number was found to decrease with increasing turbulence intensity. A correlation expression is proposed. Additional analysis with proper orthogonal decomposition was performed to enhance the understanding of complex flow structures downstream of the expansion. Finally, an overall correlation expression for the reattachment length was obtained for $500 \leq Re \leq 15\,000$ and $0.2 \leq \text{TI (\%)} \leq 20$. For a given turbulence intensity, the reattachment length can be expressed for laminar and turbulent regions as a function of the Reynolds number. The reattachment length in the transition region can be expressed as a fractional average of reattachment lengths for laminar and turbulent flows.

Published under an exclusive license by AIP Publishing. https://doi.org/10.1063/5.0095569

I. INTRODUCTION

Fluid flow through an axisymmetric sudden expansion flow system is widely observed in many fields of study, where a pipe is connected with a smaller pipe, such as the transportation of oil and gas,[1] microfluidics,[2] heat exchangers,[3] stenosis in a blood vessel,[4] and flow systems in nuclear reactors.[5] Flow behavior downstream of the expansion is complex and rich in flow physics. Flow recirculation occurs at the corner of the expansion, and spatial and temporal fluctuations (or localized turbulence) may be observed based on the upstream flow. It is crucial to understand this phenomenon from an engineering point of view as this phenomenon relates to (a) flow mixing downstream of the expansion joint; (b) energy required to transport the fluid through the piping system; and (c) the impact of flow induced vibration on the structural integrity of piping systems.

There are several experimental measurements of velocity profiles and reattachment lengths of flow through an axisymmetric expansion in the literature. Chaturvedi[6] determined the reattachment length (Lr)

and turbulent characteristics at very high Reynolds numbers ($Re = U_b d/\nu = 200\,000$) by using hot-wire anemometry to measure velocity profiles at different axial locations. Here, U_b is the bulk velocity at the entrance of the upstream pipe, d is the diameter of the upstream pipe, and ν is the kinematic viscosity of the fluid. Yang,[7] Khezzar,[8] So,[9,10] and Durrett[11] used a laser Doppler anemometer (LDA) to measure the velocity profile in a circular pipe, while Lukacs and Vad[12] measured velocity profiles in a square duct. Experiments with LDA are usually performed at a high Reynolds number ($Re > 10\,000$), resulting in a normalized reattachment length (Lr/h) between 5 and 10, regardless of the expansion ratio (ER) or the Reynolds number.[9] Iribarne[13] used fluorescent dye to measure velocity profile with UV light and a high speed camera. Back and Roschke,[14] Latornell,[15] and Pak[16] injected dye downstream of an axisymmetric expansion joint at various stream-wise locations to study reattachment.

Several efforts have been made to measure the critical value of Re that separates laminar and transition regimes. However, there is no consensus on the value of the critical Reynolds number.

Sreenivasan[17] studied the flow through an axisymmetric expansion using a hot wire anemometer. They observed fluctuations and oscillations in the flow downstream of the expansion. Mullin[18] measured the velocity profile using magnetic resonance imaging (MRI) and found the critical Reynolds number (Re_c) to be 1139. Above the critical Reynolds number, the asymmetry of velocity profiles increased with the Reynolds number, while a constant low asymmetry was observed below the critical Reynolds number. Gach[4] also measured the reattachment length by using MRI. The transition region is characterized by a decrease in the reattachment length with $Re^{-1.1}$. Furuichi[19] measured the axial velocity using an ultrasound technique, and the velocity profiles suggested that the critical Reynolds number was 1500. The ambiguity in the value of the critical Reynolds number was due to the complexity of the expansion flow in the transition region. Selvam[20] conducted numerical simulation for gradual expansion. For $Re = 1680$ or higher, with this level of disturbance as mentioned above, localized turbulence was triggered. Sanmiguel-Rojas[21] calculated the critical Reynolds number (Re_c) using the global mode analysis for a sudden expansion flow with an ER of 2. The flow became linearly unstable at a critical Reynolds number of 3273 or higher, and it corresponded to an oscillatory bifurcation with wave number $|m| = 1$ located at the end of the recirculation region, implying that localized turbulence was generated regardless of the inlet condition.

Characteristics of sudden expansion flow are usually quantified by the reattachment length (Lr). Results from both dye injection experiments of Latornell[15] and Pak[16] represent that there are three possible flow regions downstream of the sudden expansion as a function of the Reynolds number: laminar, transition, and turbulent. In the laminar region, the reattachment length is directly proportional to the flow Reynolds number (Re). For pipe flow with an ER of 2, as is investigated in this work, the correlation is found as $Lr/h = 0.0885\,Re$, where h is the step height. A similar result is also found in Fletcher's numerical simulation[22] for laminar flow, which expressed as $Lr/h = 0.0898\,Re$. The slope of this correlation is dependent on the ER with a larger ER is giving a smaller slope. In these cases, the upstream Reynolds number is defined as $U_b d/\nu$, where U_b is the bulk velocity at the inlet, d is the diameter of the upstream pipe, and ν is the kinematic viscosity of the fluid.

As the Reynolds number increases and exceeds a certain threshold value, the relationship between reattachment length and Reynolds number reverses with the reattachment length decreases with an increase in the Reynolds number. The stratified flow becomes unstable and collapses shorter distance downstream than in laminar flows due to localized turbulence. One explanation for this is that the Kelvin–Helmholtz instability is initiated between the mainstream and recirculation flows due to the velocity difference as the Reynolds number is increased. As the Reynolds number increases further, the reattachment length becomes less dependent on the Reynolds number and can eventually be considered independent of the Reynolds number, converging to an asymptotic value. Moallemi and Brinkerhoff[23] estimated the reattachment length for the sudden expansion flow as a function of the Reynolds number using the Direct Numerical Simulation (DNS) technique, but their results overestimated the reattachment lengths in the transition region compared with the experimental data reported in the literature.[15,16]

In addition to the Reynolds number, the reattachment length is also affected by the shape of the inlet flow profile, and the turbulent

intensity at the flow inlet. It is difficult to study the effect of flow disturbance because it is hard to maintain the exact desired amount of the disturbance, and unexpected disturbances from external sources (i.e., pumping systems) can impact the flow. So[9] reported that there is a clear trend on the reattachment length as a function of parameter $u_{rms}/\bar{U}_m$. For $2.5\% < u_{rms}/\bar{U}_m < 17.5\%$, the reattachment length decreases as $u_{rms}/\bar{U}_m$ increased.[6,7,9–11] Here, u_{rms} is the root mean square of fluctuation velocity, and $\bar{U}_m$ is the averaged bulk velocity.

Latornell[15] conducted a dye injection experiment for flow in a circular pipe and concluded that the reattachment length depends on the shape of the inlet profile. The reattachment length with a plug profile at the inlet [high turbulence kinetic energy (TKE)] is shorter than that for the case of a fully developed inlet velocity profile. Pak[16] mentioned that the reattachment length is sensitive to artificially induced disturbances, such as small vibrations in the inlet feed line or from the test bench during the experiment. The reattachment length longer than $30h$ broke down quickly when a small external disturbance was applied.

Numerical simulation studies[5] showed that the shape of the velocity profiles is very different in the absence of any artificial disturbance when compared to the experimental results reported in the literature.[15,16,18,19] Without artificial disturbances, the reattachment length trend may follow the trend of the laminar flow at the higher Reynolds numbers ($Re = 2000$). There are a lot of numerical[20,24–28] and experimental[29] studies about the amplitude threshold of flow disturbance (or critical value). Sanmiguel-Rojas[24] and Selvam[20] showed a small flow perturbation perpendicular to the main flow, impacting both the magnitude and location of the onset of instability in their DNS study. The method used to generate an artificial disturbance at inlet is one of the independent parameters for this study. A small constant distortion of amplitude δ was applied to the fully developed laminar flow $U_r = 2(1 - 4r^2)$, giving an inlet velocity $\boldsymbol{U}_{in}$ of

$$\boldsymbol{U}_{in} = 2(1 - 4r^2)\mathbf{e}_z + \delta\mathbf{e}_y, \tag{1}$$

where r is the radial coordinate, $\mathbf{e}_z$ is the axial coordinate vector, and $\mathbf{e}_y$ is the traverse coordinate vector.

Selvam,[20] Lebon,[25] Nguyuen,[26] and Shenoy,[27] on the other hand, applied a simple localized perturbation at the inlet in the form of a vortex. Nguyen[26] introduced a vortex perturbation in a DNS model of a sudden expansion flow and showed that the critical amplitude for vortex perturbation is proportional to Re^{-3}. Shenoy[27] studied flow through a gradual expansion, and the critical amplitude was found to be proportional from $Re^{-2.1}$ to $Re^{-4.6}$ for a gradual angle θ from $45°$ to $4.76°$, respectively, and the resulting equation for the inlet velocity is

$$\boldsymbol{U}_{in} = U(r)\mathbf{e}_z - y\delta\Omega\mathbf{e}_x + x\delta\Omega\mathbf{e}_y, \tag{2}$$

$$\Omega = \begin{cases} 1, & s \le \Re/2, \\ 2(\Re - s)\Re, & \Re/2 < s \le \Re, \\ 0, & s > \Re, \end{cases} \tag{3}$$

where $U(r)$ is the base axial velocity profile at the inlet, δ and Ω are the amplitude and the intensity of the vortex perturbation, respectively, $\Re$ is the radius of the vortex, and $s = \sqrt{(x - x_0)^2 + (y - y_0)^2}$ is the distance between the center of the vortex (x_0, y_0) and any point (x, y) in the cross section.

However, the methods mentioned above have limited applicability because in reality, it is not practical to reproduce and control the flow disturbance. The introduction of flow disturbance with a random variable can be an alternative. The strength of this method is that the amount of disturbance can be correlated with turbulence intensity ($u_{rms}/\bar{U}_m$), which is a widely employed turbulence property, enabling direct comparison with the experimental data in the literature. Current and previous[5] studies employed this inlet boundary condition [Eq. (5)], considering both randomized disturbance and the velocity of the previous time step. Luciano[28] employed similar concept that only considered a random disturbance, which is written as follows:

$$\boldsymbol{U}_{in} = \boldsymbol{U}_{ref} + \delta|\boldsymbol{U}_{ref}|(2\mathbb{R}), \qquad (4)$$

where $\boldsymbol{U}_{ref}$ is the reference velocity (fully developed laminar flow) and $\mathbb{R}$ is the random function between –0.5 and 0.5.

Various studies on flow through an axisymmetric expansion mentioned above are summarized in Table I.

The present study builds upon the results reported in the literature. The unique features of this work are as follows: (a) turbulence intensity was used to characterize the flow disturbance at the inlet; (b) large eddy simulation (LES) with the WALE model[30] was used to study the flow characteristics through an axisymmetric sudden expansion; (c) the numerical results generated as part of this study match the experimentally measured values of reattachment lengths in the

laminar, transition, and turbulent flow regimes with physically reasonable turbulence intensity; (d) new classification of the flow characteristics for flow through a sudden expansion is suggested, and a correlation expression for the critical Reynolds number is developed; (e) using the generated numerical data, a correlation was developed for reattachment length (Lr) as a function of the Reynolds number (Re) and turbulence intensity (TI) at the inlet for the ER value of 2.0; and (f) Proper Orthogonal Decomposition (POD) analysis was performed to gain deeper understanding of the characteristics of flow through an axisymmetric expansion.

II. NUMERICAL PROCEDURE
A. Geometry, inlet conditions, and mesh

Figure 1 illustrates the geometry of the axisymmetric sudden expansion used in the current study, comprised of two different sizes of concentric pipe with inner diameters of 25 mm for upstream (d) and 50 mm for downstream (D), yielding ER = 2. The upstream length from the sudden expansion is set to $5d$ to minimize the attenuation of turbulent energy for laminar flows, while the length of the downstream pipe is set to $40d$ or more to minimize the exit effects on the reattachment length.

A fully developed parabolic velocity profile for laminar flow is specified as a base boundary condition at the inlet. To introduce the turbulent disturbance on the flow, a randomly generated fluctuation

TABLE I. Summaries of papers about flow through an axisymmetric sudden expansion in the transitional region.

| Name	ER	Method	Measured properties	Re_C (Lr_C)	Correlation
Iribarne et al.[13]	2.0	Dye	Reattachment length	296 (27.0)	$Lr \sim Re^{-0.77}$
Latornell and Pollard,[15] FD	2.0	Dye	Reattachment length	915 (86.5)	$Lr \sim Re^{-2.012}$
Latornell and Pollard,[15] NZ	2.0	Dye	Reattachment length	617 (40.8)	$Lr \sim Re^{-1.993}$
Sreenivasan and Strykowski[17]	2.0	Hot wire	Flow characteristics	1500–1700	
Fletcher et al.[22]	2.0	NS	Reattachment length	$\cdots$	$Lr/h = 0.089\,8Re$ (laminar)
Pak et al.[16]	2.0	Dye	Reattachment length	688 (50.0)	$Lr \cong 1.321 \times 10^{10}\,Re^{-3.003} + 10.43$
Gach and Lowe[4]	2.0	MRI	Reattachment length	526 (24.0)	$Lr \sim Re^{-1.07}$
Furuichi et al.[19]	1.8	UVP	POD study	1500	$\cdots$
Mullin et al.[18]	2.0	MRI	Asymmetry	1139	$\cdots$
Sanmiguel-Rojas et al.[21]	2.0	$\cdots$	Global mode analysis	3273	$\cdots$
Sanmiguel-Rojas and Mullin[24]	2.0	DNS	Amplitude threshold curves	1500	$\delta \sim Re^{-0.006}$
Selvam et al.[20]	2.0	DNS	Asymmetry of flow field	912	$\cdots$
Selvam et al.[20]	2.0	DNS	Friction coefficient	1680	$\cdots$
Selvam et al.[31]	2.0	DNS	POD study	$\cdots$	$\cdots$
Howard et al.[32]	2.0	LES	POD study	$\cdots$	$\cdots$
Lebon et al.[29]	2.0	PIV	Amplitude threshold curves	$\cdots$	$V_{r,c} \sim Re^{-2.3}$
Lebon et al.[25]	2.0	DNS	Amplitude threshold curves	$\cdots$	$\delta \sim Re^{-2.8}$
Moallemi and Brinkerhoff[23]	2.0	DNS	Reattachment length	1003 (81.7)	$Lr \cong 3.537 \times 10^7\,Re^{-2.03} + 52.84$
Nguyen et al.[26]	2.0	DNS	Amplitude threshold curves	$\cdots$	$\delta \sim Re^{-3}$
Shenoy et al.[27]	2.0	DNS	Amplitude threshold curves	$\cdots$	$\delta \sim Re^{-2.1}$–$\delta \sim Re^{-4.6}$
Luciano et al.[28]	2.0	DNS	Amplitude threshold curves	$\cdots$	$\delta \sim Re^{-9.6}$
Luciano et al.[28]	2.0	DNS	Reattachment length	$\cdots$	$\cdots$
Choi et al.[5]	2.0	LES	Reattachment length	816 (69.4)	$Lr \cong 4.646 \times 10^6\,Re^{-1.672} + 7.471$
Current study	2.0	LES	Reattachment length	Eq. (13)	Eqs. (15)–(18)
Current study	2.0	LES	POD study	Table III	
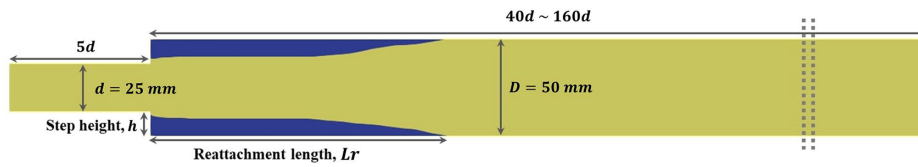
FIG. 1. Schematic geometry for the axi-symmetric sudden expansion flow. Blue-colored area is the region where axial velocity is negative.

velocity based on turbulence intensity (TI) is appended to the boundary condition at the inlet. Turbulence intensity is defined as the ratio of the fluctuation velocity to the mean velocity ($u_{rms}/\bar{U}_m$). The in-house coded boundary condition based on *turbulentInlet* of the OpenFOAM v7 is employed as an inlet boundary condition for the simulation. The velocity equation at the inlet is written as

$$\boldsymbol{U}_{in} = (1 - \alpha)\boldsymbol{U}_{old} + \alpha(\boldsymbol{U}_{ref} + C_{rms}|\boldsymbol{U}_{ref}|I\mathbb{R}), \quad (5)$$

$$\boldsymbol{U}_{ref} = 2U_b(1 - (r/R)^2)\,\mathbf{e_z}, \quad (6)$$

where $\boldsymbol{U}_{in}$ is the velocity at the inlet, $\boldsymbol{U}_{old}$ is the inlet velocity of previous time step, $\boldsymbol{U}_{ref}$ is the reference velocity, $|\boldsymbol{U}_{ref}|$ is the magnitude of the reference velocity, α is the fraction of new random component added to the previous time value and is specified as 0.1 in the current study, C_{rms} is the RMS coefficient, defined as $\sqrt{12(2\alpha - \alpha^2)/\alpha}$ and specified as 15.10 in the current study, $\mathbf{e}_z$ is the axial coordinate vector, r is the radial location, R is the radius of pipe, U_b is the bulk velocity, I is the turbulence intensity, and $\mathbb{R}$ is an equally distributed random variable between −0.5 and 0.5.

The blue color in Fig. 1 represents a region in which the flow reversal of averaged axial velocity exists. The time-averaged velocity profiles adjacent to the wall are extracted parallel to the axis every 5° sections to calculate the reattachment point and averaged.

The mesh used in the current study is shown in Fig. 2. Grid information follows a previous study of the author.[5] Grid independence was established by monitoring the Grid Convergence Index[33] (GCI), and grid independence was declared when the GCI ceased to vary by more than 1%. The mesh size in the axial direction was kept constant at 3.33 mm, equivalent to $\Delta z^+ = 11.82$, 29.50, and 45.6 for $Re = 1000$, 3000, and 5000, respectively. The cross-sectional mesh has non-uniformly sized 1536 cells as illustrated in Fig. 2(a). The smallest mesh element adjacent to the wall in the upstream pipe section is specified as 7.20×10^{-5} m, whereas in the downstream section, it is 1.03×10^{-4} m. The cell sizes in the vicinity of the wall were small enough to resolve finer gradients and were of the order of $y^+ = 1$,

which is equivalent to 2.82×10^{-4}, 1.13×10^{-4}, and 0.731×10^{-4} m for $Re = 1000$, 3000, and 5000, respectively. Figure 3 represents the size of meshes in the radial direction for different Reynolds numbers.

B. Settings for OpenFOAM

Time-dependent computational fluid dynamics (CFD) simulations were conducted using OpenFOAM v7, an open-source CFD simulation program. Each case was run for 48 h or more with 48 CPUs on GRACE, comprised of the Intel Xeon 6248R processor, in the high performance research computing center of Texas A&M University. The pimpleFOAM solver was employed. The pimpleFOAM iteration settings, nOuterCorrectors, nCorrectors, and nNonOrthogonalCorrectors, were set as 5, 2, and 1, respectively. Convergence at each time step is achieved when the residual of each property was less than 1×10^{-5} except for the final loop, where the criterion was 1×10^{-6}. A second-order backward difference scheme was used to calculate the temporal derivatives. The Linear-Upwind Stabilized Transport (LUST) scheme was used to calculate the first order spatial derivative of velocity, and the second-order central difference scheme was used to compute other spatial derivatives. Simulation runs were made for 24 s or more, and the temporally averaged velocity and turbulence quantities were calculated. Information obtained during the first one-third of data was excluded from the calculation of the average of properties.

The effect of time step was investigated for the Reynolds number of 1300 with three different turbulence intensities (TI = 0.1%, 1%, and 10%). Figure 4 shows the dependence of the reattachment length on time step. Based on GCI calculations [GCI = $(F_s\varepsilon/(r^p - 1))$], a minimum time step of 5×10^{-4} s was required to maintain 7% relative error for the case of TI = 0.1%. A summary of time step independence studies is given in Fig. 4 and Table II. Here, F_s is the safety factor of 1.25, ε is the relative error of the reattachment length between two different meshes, r is the ratio of the mesh size, and p is the order of convergence. Time steps (Δt) for $Re \leq 1600$, $1600 \leq Re \leq 5000$, and $5000 \leq Re \leq 15\,000$ were determined to be 5×10^{-4}, 4×10^{-4}, and 2×10^{-4} s, respectively.
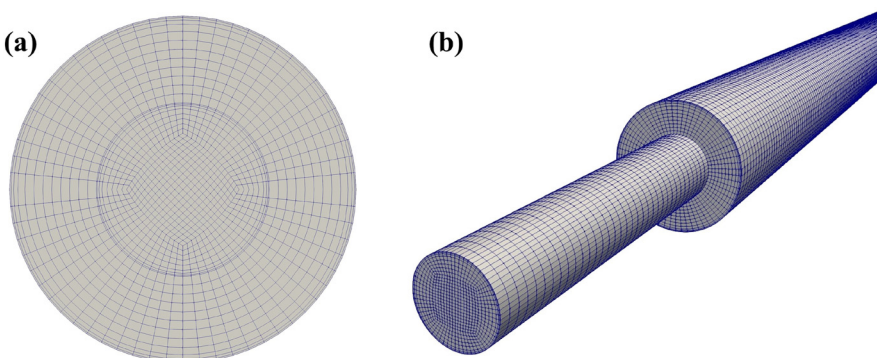

(a)   **(b)**

FIG. 2. Mesh used in present study: (a) cross-sectional view of the mesh at the outlet and (b) three dimensional view near the sudden expansion.
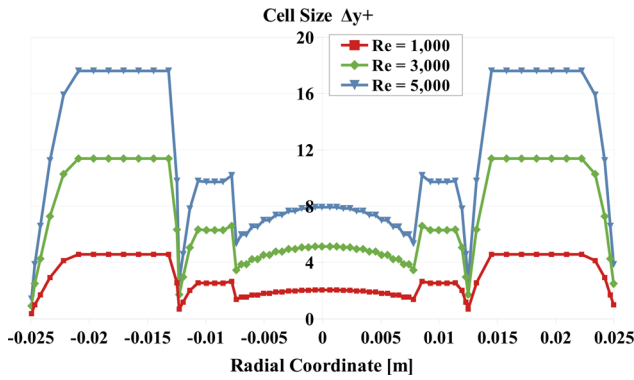
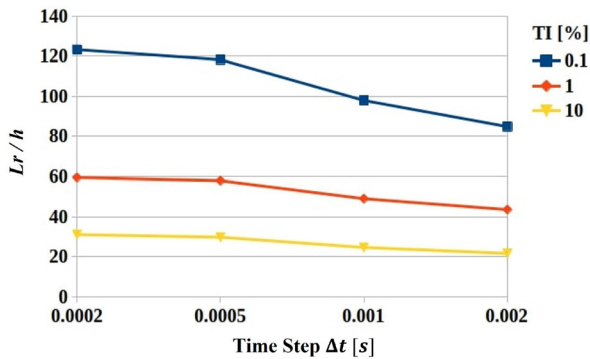**FIG. 3.** Size of meshes in the radial direction for $Re = 1000$, 3000, and 5000.

FIG. 4. Dependence of the reattachment length on time step.

TABLE II. Grid convergence test for time step ($Re = 1300$). Subscripts 1, 2, and 3 represent $\Delta t = 0.0002$, 0.0005, and 0.001 s, respectively.

TI (%)	0.1	1.0	10
GCI_{12}	1.651	0.661	1.820
GCI_{23}	6.998	3.973	7.414

The normalized time step $\Delta t^+ = \Delta t/(h/U_b)$ is 0.025 72, 0.061 74, and 0.102 9 for $Re = 1000$, 3000, and 5000, respectively.

In this study, the maximum Courant number varied from 0.1 to 5 depending on the Re, TI, and time step. However, only a small number of cells experienced a Courant number larger than unity. Furthermore, in all cases, the convergence criterion of 1×10^{-6} was met, and the GCI criteria was used for different time steps to declare convergence. Most importantly, with the current mesh size and the time step size, we were able to reproduce results for reattachment length similar to the literature[15,16,28] to validate the current numerical simulation.

C. Large eddy simulation (LES)

The LES approach resolves large scale flow structures and models small scale flow structures as they are universal. For incompressible flow, the Navier–Stokes equation for LES is as follows:

$$\frac{\partial \tilde{U}_i}{\partial t} + \frac{\partial}{\partial x_j}(\tilde{U}_i \tilde{U}_j) = -\frac{1}{\rho}\frac{\partial \tilde{p}}{\partial x_i} + \nu \frac{\partial^2 \tilde{U}_i}{\partial x_j^2} + \frac{1}{\rho}\frac{\partial \tau_{ij}}{\partial x_j}, \quad (7)$$

$$\tau_{ij} = -\frac{2}{3}k_{sgs}\delta_{ij} + 2\nu_{sgs}\tilde{S}^*_{ij}, \quad (8)$$

where $\tilde{U}_i$ is the filtered instantaneous velocity, $\tilde{p}$ is the filtered pressure, τ_{ij} is the residual stress tensor, ν_{sgs} is the subgrid-scale viscosity, k_{sgs} is the subgrid-scale turbulence kinetic energy, which can be calculated by $\nu_{sgs} = C_k \Delta \sqrt{k_{sgs}}$, C_k is a constant, Δ is the sub-grid characteristic length scale, $\tilde{S}^*_{ij}$ is the deviatoric tensor of the filtered strain rate, and δ_{ij} is the Kronecker delta.

In this study, an LES with the WALE model proposed by Nicoud and Ducros[30] was adopted. In this model, subgrid eddy-viscosity is proportional to the cube of wall-normal component ($\nu_{sgs} \sim y^3$) and goes to zero near the wall; hence, neither constant adjustment nor damping function is required for wall-bounded flows. They revised the Smagorinsky eddy-viscosity model by employing the velocity gradient tensor $\tilde{g}_{ij} = \frac{\partial \tilde{U}_i}{\partial x_j}$, yielding the subgrid-scale viscosity model as follows:

$$\nu_{sgs} = (C_w \Delta)^2 \frac{(S^d_{ij} S^d_{ij})^{1.5}}{(\tilde{S}_{ij} \tilde{S}_{ij})^{2.5} + (S^d_{ij} S^d_{ij})^{1.25}}, \quad (9)$$

where ν_{sgs} is the subgrid-scale viscosity, C_w is a constant, Δ is the subgrid characteristic length scale, S^d_{ij} is the traceless symmetric part of the square of the velocity gradient tensor, defined as Eq. (10), and $\tilde{S}_{ij}$ is the filtered strain rate, defined as Eq. (11),

$$S^d_{ij} = \frac{1}{2}(\tilde{g}^2_{ij} + \tilde{g}^2_{ji}) - \frac{1}{3}\delta_{ij}\tilde{g}^2_{kk}, \quad (10)$$

$$\tilde{S}_{ij} = \frac{1}{2}\left(\frac{\partial \tilde{U}_i}{\partial x_j} + \frac{\partial \tilde{U}_j}{\partial x_i}\right). \quad (11)$$

No partial differential equation for either Reynolds stress, subgrid-scale viscosity, or the dissipation rate is required because the WALE model is an algebraic eddy viscosity model. This modified eddy-viscosity model allows simulating both laminar and turbulent regions of flows in a pipe. As the model produces zero eddy-viscosity in the case of pure shear, the laminar to turbulent transition process can be reproduced.

Li[34] conducted LES with the WALE model to reproduce the turbulent flows of twin parallel jets and observed good agreement with Particle Imaging Velocimetry (PIV) measurements. Choi[5] also compared the result of an LES model with the PIV measurements made in the Low Pressure Low Temperature (LPLT) Fission Product Venting System (FPVS) test facility and found a reasonable agreement. Therefore, the WALE LES model was selected to study turbulent flow in this study.

D. Proper orthogonal decomposition (POD)

The proper orthogonal decomposition (POD) refers to a modal decomposition technique in which a set of data are expressed as a linear summation of a set of orthonormal modes with corresponding temporal coefficients.[35] Each mode is expected to describe a feature of the system. POD analysis was first introduced by Lumley[36] in the field of fluid dynamics/turbulent flows to capture the coherent structure in a temporally oscillating and spatial fluctuating turbulent flows. The set

of velocity profiles in a time series can be expressed as a linear summation of the mode with corresponding temporal coefficient written as Eq. (12). Each mode is expected to have a coherent structure of the fluctuating flow. Since this technique enables the decomposition of a set of data into a minimal number of modes to capture as much as energy (information) as possible, velocity profiles can be expressed a sum of minimum number of modes. The method of snapshot[37] is employed to calculate eigenvalue, temporal coefficient, and mode,

$$U(\boldsymbol{x}, t) - \bar{U}(\boldsymbol{x}, t) = \sum_{i=1}^{N} \zeta^{(i)}(t)\psi^{(i)}(\boldsymbol{x}), \qquad (12)$$

where $U(\boldsymbol{x}, t)$ is the instantaneous velocity, $\bar{U}(\boldsymbol{x}, t)$ is the temporally averaged velocity, $\zeta^{(i)}(t)$ is the temporal POD coefficient, and $\psi^{(i)}(\boldsymbol{x})$ is the mode. The order of the mode is determined by the eigenvalue $\lambda^{(i)}$ in descending order, representing their energy level.

III. RESULTS AND DISCUSSION

A. Critical points to demarcate laminar, transition, and turbulent regions

Large eddy simulations were performed for different Reynolds numbers for the geometry of axisymmetric pipes. The reattachment length normalized by the step height (Lr/h) in the pipe flow is presented in Fig. 5 as a function of the Reynolds number. Solid markers represent data reported in the literature.[15,16,23,28] Hollow markers are the data obtained from the current LES calculations with different turbulence intensities. Error bars represent the range of the reattachment length in the circumferential direction. The dashed line is the universal correlation for the reattachment length proposed in this study for a given turbulence intensity [Eq. (17)].

In the absence of disturbance at the inlet, the reattachment lengths obtained from the numerical simulation maintain the trend of the laminar flow region, wherein the reattachment length is linearly proportional to the Reynolds number. This trend, however, is shown to change around $Re = 2000$ wherein the reattachment length is no longer linearly proportional to the Reynolds number and becomes nearly independent of the Reynolds number, as seen in the left top corner inset of Fig. 5. With assigned numerical convergence of 1×10^{-6},

the numerical error can generate flow fluctuation. As the magnitude of flow disturbance due to the absolute numerical error is maintained regardless of the Reynolds number unlike the turbulent intensity disturbance, the reattachment length does not change regardless of the Reynolds number in the turbulent region.

With a proper amount of turbulence disturbance introduced as Eq. (5), the reattachment length calculated from the current study is in good agreement with data reported in the literature. Latornell and Pollard[15] performed experiments with two different inlet conditions: fully developed flow (FD) depicted as a green square and nozzle flow (NZ) depicted as a red circle in Fig. 5. For the FD case, the inlet velocity profile is controlled by the parabolic fully developed laminar flow by introducing a very long upstream ($> 40d$). It is expected that turbulence intensity is low at the entrance of the expansion as flow disturbances at the inlet are attenuated as fluid flows through the pipe for cases for which the Reynolds number was less than 2000. Nozzle flow, on the contrary, employed a short nozzle upstream of the expansion and was measured as plug flow in which the turbulence intensity was expected to be high. This trend is consistent with the current study. Both the FD and NZ cases of Latornell and Pollard[15] match the current study with turbulence intensities of 1% and 20%, respectively. Similarly, Pak[16] also used the short nozzle upstream of the expansion and fit well on the turbulence intensity of 20%. The current results are consistent with the explanation given by So[9] that the reattachment length decreases as the turbulence intensity increases. Moallemi[23] performed a DNS study using a different method to introduce disturbance at the flow inlet. The decreasing rate at transition and turbulent regions do not agree with the numerical results of the current study. Luciano et al.[28] also performed DNS study, showing a similar decreasing rate compared with the experimental data[15] and current LES result. Luciano's DNS study with $\delta = 5\%$ matches the present study with TI = 1%, while the case with $\delta = 1\%$ matches current study with TI = 0.2%. It appears that δ is five times larger than TI. TI is the range of a random variable, whereas δ is the amplitude of the random variable used in Eq. (4). The range of random variable is half of the amplitude of the random variable, and thus, two times difference is attributed to this. Another reason δ appears larger than TI is due to
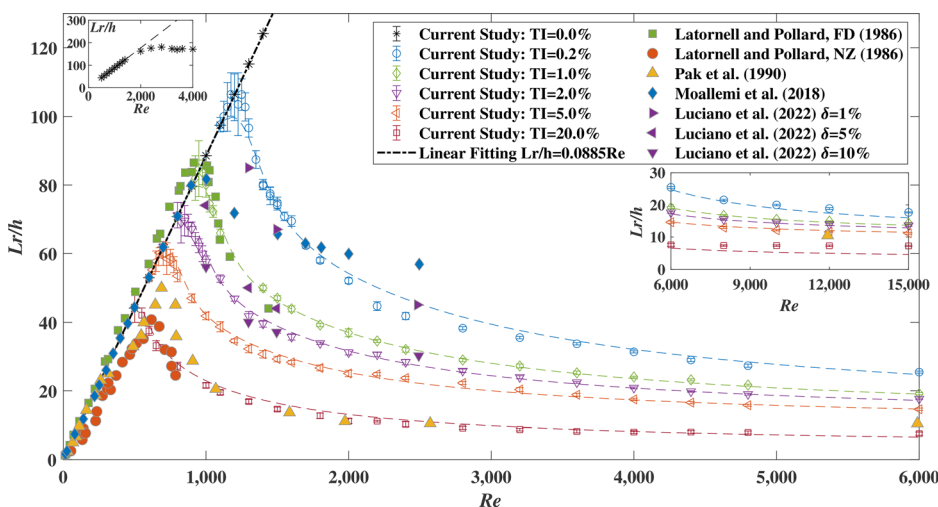

FIG. 5. Comparison of normalized reattachment length (Lr/h) for the axisymmetric pipe as a function of the Reynolds number.
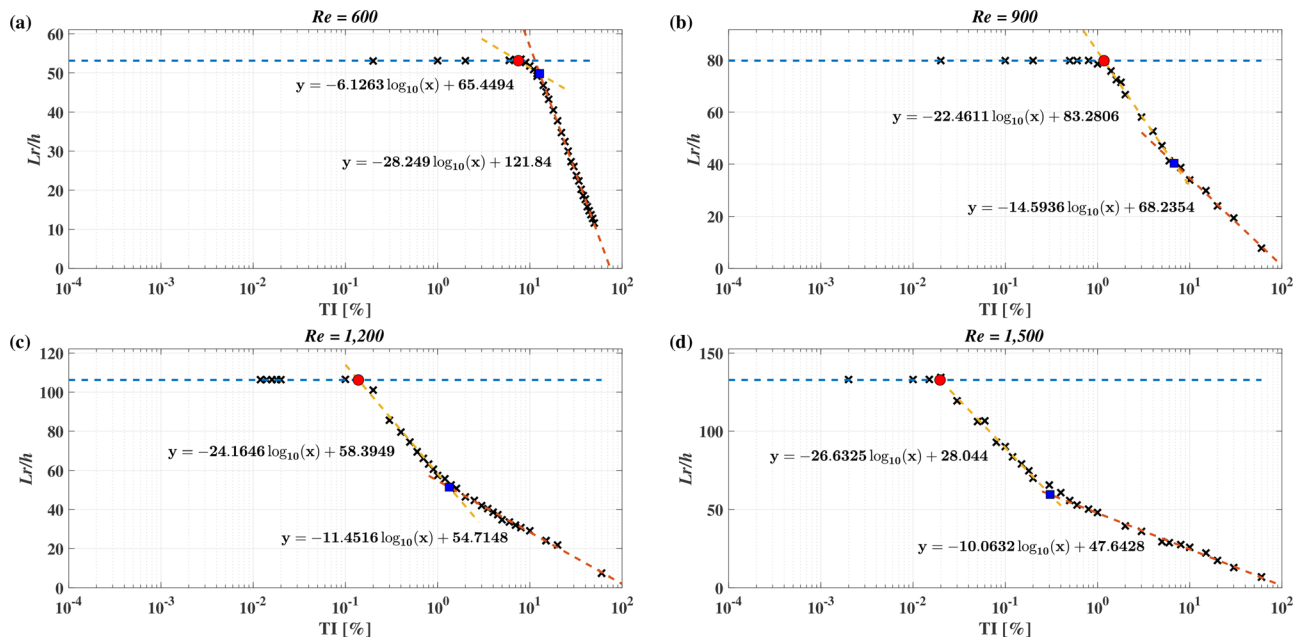
FIG. 6. The reattachment length (Lr) as a function of turbulence intensity (TI) for constant Re: (a) $Re = 600$, (b) $Re = 900$, (c) $Re = 1200$, and (d) $Re = 1500$.

the fact that the present study considered information of the previous time step, while Luciano's study[28] does not.

Flow characteristics are clearly classified on the graph of reattachment length as a function of the turbulence intensity in Fig. 6. The marker X on the graphs in Fig. 6 indicates the reattachment length calculated from the numerical simulation with different turbulence intensities for a specified Reynolds number. Plots of the reattachment length as a function of turbulence intensity have three distinct parts: a region in which the reattachment length has constant value, and two regions described by lines with different negative slopes on a semi-log x-axis scale plot. Flow is not affected by flow disturbance at the inlet in the laminar region as shown by the constant blue lines in Fig. 6. On the contrast, in transition and turbulent regions, flow behavior depends on the flow disturbance at the inlet. The magnitude of the slope of the second region (yellow line) is lower than that of the third region (red line) for $Re \leq 800$, as shown in Fig. 6(a), while it is opposite for cases with $Re > 800$, as shown in Figs. 6(b)–6(d). Three regions make two crossover points (Cr_1 and Cr_2) between adjacent lines, which are critical points that distinguish laminar-transition (red circle, Cr_1) and transition-turbulent regions (blue square, Cr_2). To obtain the relationship between the critical Reynolds number and critical turbulent intensity, parametric studies were performed by varying Reynolds number from 500 to 2000. The critical points obtained are shown in Fig. 7. Dashed lines are curve fitting expressions for the results of the parametric study. The relation between the critical Reynolds number (Re_{Cr_1}, Re_{Cr_2}) and critical turbulent intensity (TI_{Cr_1}, TI_{Cr_2}) is shown in Eqs. (13) and (14). Critical point dividing the laminar-transition region (Cr_1)

$$Re_{Cr_1} = 151.71 \ln\left(540.84/\mathbf{TI}_{Cr_1}[\%]\right). \qquad (13)$$

Critical point dividing the transition-turbulent region (Cr_2)

$$Re_{Cr_2} = 217.45 \ln\left(231.74/\mathbf{TI}_{Cr_2}[\%]\right). \qquad (14)$$

B. Flow behavior in the transitional region

Oscillation of flow is an interesting behavior in the transitional region, as shown in Fig. 8. Figure 8(a) shows a contour plot of temporally averaged axial velocity, Fig. 8(b) shows the mode 1 achieved from POD analysis using fluctuation velocity, and Figs. 8(c)–8(i) are contour graphs of instantaneous velocity as a function of time. Around the reattachment point, separated shear layers suddenly break down in the middle region, and the shear layer shortens while the downstream breakaway region disappears. Then, separated shear layers are
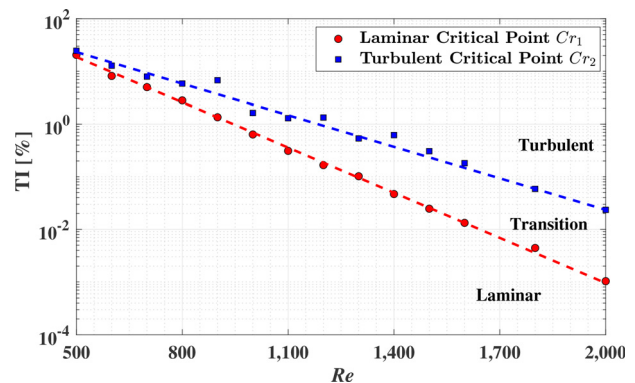

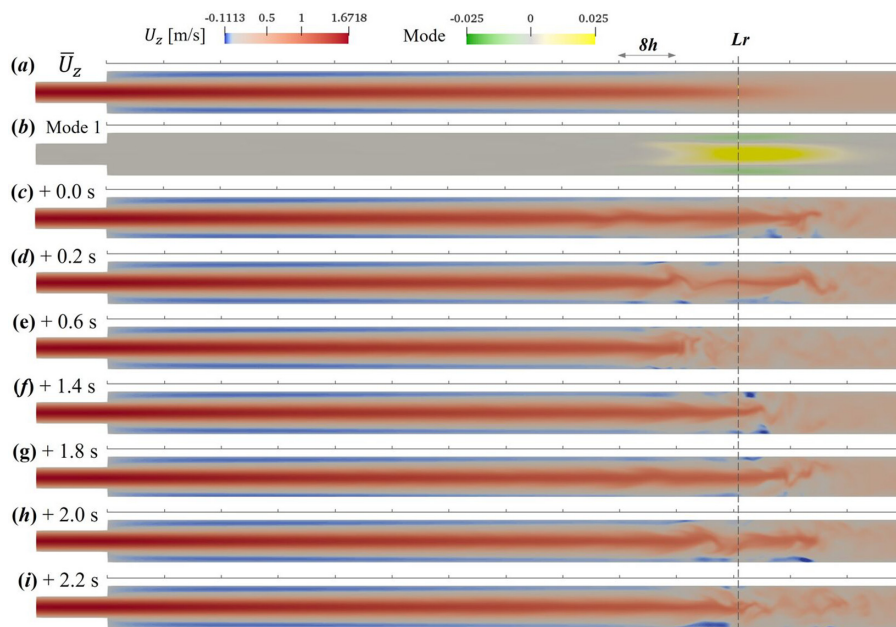**FIG. 7.** Flow map showing laminar, transition, and turbulent regions.

FIG. 8. Flow oscillation over time for a flow with the inlet condition of $Re = 1300$ and $TI = 0.2\%$: contour of (a) averaged axial velocity, (b) mode 1 of POD analysis, and (c)–(i) instantaneous velocity at the time of $+0.0$, $+0.2$, $+0.6$, $+1.4$, $+1.8$, $+2.0$, and $+2.2$ s, respectively.

elongated and recovered over time. This flow phenomenon repeats with time. The spatial range of flow oscillation is similar to the first mode of the fluctuation velocity near the reattachment length.

Asymmetricity is the another interesting flow behavior in the transitional region. It can be seen from the error bars in Fig. 5 that the asymmetric reattachment length is observed around the circumference near critical points (Cr_1) even though the fluid flows through an axisymmetric sudden expansion. Reattachment lengths presented in Fig. 5 are based on integration over 16 s; however, the calculations were carried out for 100 s to verify whether asymmetry still remained. The asymmetric reattachment is severe near the laminar critical point (Cr_1). The asymmetric reattachment length is also observed in the parallel plate channel expansion flow when the Reynolds number exceeds the critical number.[23,38] A second critical point Cr_2 is the crossover point of two curve fitted lines with different negative slopes observed in the TI vs Lr graph (Fig. 6). The key characteristics of this critical point are that the reattachment length obtained above this critical Reynolds number (Cr_2) can be represented by an expression $Lr \sim 1/Re$ regardless of turbulence intensity at the inlet.

The fast Fourier transform analysis was performed for two different inlet conditions: the transition case of $Re = 1000$ with $TI = 2\%$ in Figs. 9(b)–9(d) and the turbulent case of $Re = 2000$ with $TI = 20\%$ in Figs. 9(f)–9(h). The calculations at which fluctuation velocities are extracted are marked in Figs. 9(a) and 9(e) showing contour of averaged axial velocities. The markers $\times$, $\triangle$, and $\bigcirc$ lie at the mesh adjacent to the wall (1.999h away from the axis), at 1.2h away from the axis, and on the axis, respectively. The slope of $-5/3$ is plotted as a solid line, whereas that of -4 is done as a dashed line. The FFT results showed the slope of $-5/3$ in mid frequency range where energy cascade occurs. The FFT results also present the slope of -4 in high frequency range where energy is dissipated. These trends are especially observed downstream of the reattachment point where turbulence is

well developed. The blue line in Figs. 9(b)–9(d) and the orange line in Figs. 9(f)–9(h) are FFT results obtained near the reattachment length where flow oscillation and fluctuation are most severe, demonstrating that it has more small eddies than at other locations. The FFT results obtained at some points near the expansion, such as point $(0, 1.999h, 16h)$ and $(0, 1.999h, 40h)$ in Fig. 9(b) and point $(0, 1.999h, 40h)$ in Fig. 9(d), do not follow the turbulent process mentioned above. Instead, only slope of -4 is observed. It seems that turbulence kinetic energy is dissipated before they are fully evolved and cascaded to smaller eddies. This can be considered as the characteristics of transition flow in an axisymmetric expansion.

C. Result of proper orthogonal decomposition study

To identify the coherent structure of the flow in an axisymmetric sudden expansion, the 2D (axial and transverse) POD analysis was performed. Eigenmode and eigenvalue are used to classify the flow characteristics in axisymmetric sudden expansion flows. Data were sampled in every 2×10^{-3} s for a period of 50 s giving 25 000 snapshots. Figure 10 represents the first mode obtained from POD analysis of axial fluctuation velocity for different Reynolds numbers at a fixed inlet turbulence intensity ($TI = 2\%$). Note that Fig. 10 shows the first Eigen mode (mode 1) of the fluctuating axial velocity not the actual fluctuation velocity itself. The red and blue colors indicate positive and negative modal values, respectively. The temporal coefficients could either be positive or negative and may change with time. However, the positive and negative values of mode 1 presented in Fig. 10 do not indicate the direction of flow. Four different patterns of the first mode were observed: (p1) alternating pattern on the zero shear layer ($Re \leq 725$); (p2) single directional strong spot pattern with twin tip ends where localized turbulence was observed ($750 \leq Re \leq 1,200$); (p3) strong spot pattern with single tip end accompanied by twin-tail-like pattern (in blue) in opposite directions ($1300 \leq Re \leq 2800$); and
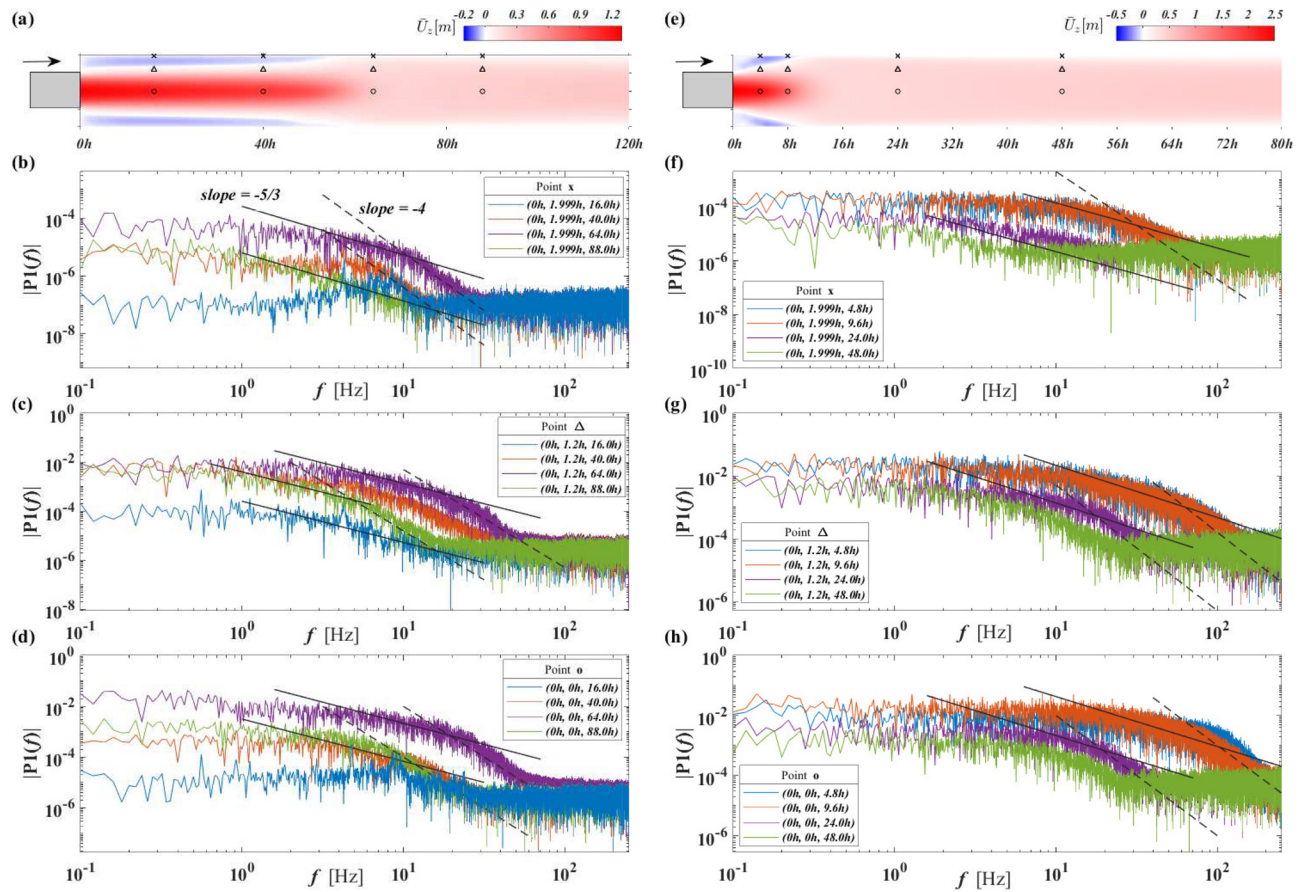
FIG. 9. Fast Fourier transform analysis of axial fluctuating velocity at different locations: (a)–(d) transition case of $Re = 1000$ with TI = 2%, (a) contour of averaged axial velocity, (b)–(d) FFT results adjacent to the wall ($\times$), at $y = 1.2h$ from the axis ($\triangle$), and on the axis ($\bigcirc$), respectively; (e)–(h) turbulent case of $Re = 2000$ with TI = 10%, (e) contour of averaged axial velocity, (f)–(h) FFT results adjacent to the wall ($\times$), at $y = 1.2h$ from the axis ($\triangle$), and on the axis ($\bigcirc$), respectively.

(p4) single vortex spot (Re $\geq$ 3200). Note the color legend in Fig. 10 is only employed for showing relative direction in the same mode. As a sign in the temporal POD coefficient is temporally oscillating, axial velocity due to this mode can move either forward or backward. Pattern (p1) can be treated as a laminar flow where strongest fluctuation of the flow characteristics is induced by the Kelvin–Helmholtz instability on the zero shear layer, whereas a strong mode spot is observed on the place where separated shear layers breakdown on pattern (p2), (p3), and (p4), which can be considered as localized turbulence near the reattachment point. Since the sign of values in the first mode of patterns (p2) and (p3) is biased to certain directions, the length of the separated shear layer is based on temporal coefficients explaining the temporal oscillation of the flow downstream of the expansion. On the contrary, in the pattern (p4), flows are not oscillating because half negative and positive values of mode 1 coexist.

This POD analysis was performed for different turbulence intensity values (TI = 0%, 2%, 0.5%, 1%, 2%, 5%, 10%, and 20%). The results are tabulated in Table III and employed to study the flow characteristics. The contour of mode 1 for each turbulence intensity can be accessed in the supplementary material. The interface between each

pattern can be considered as the critical value of Re corresponding to reattachment length. The interface between patterns p1 and p2 of mode 1 corresponds to Cr_1 obtained from Eq. (13). The critical value decreases as turbulence intensity increases. This critical value from mode 1 is slightly smaller than what was obtained by tracking the reattachment length (Fig. 5). It is consistent with the flow physics as the reattachment length is the result of the competition between recirculation due to laminar flow characteristics and localized turbulent flow characteristics. Similarly, the p2/p3 interface is a candidate for Cr_2, but it is not distinct because patterns p2 and p3 look similar and are, thus, hard to classify clearly. In addition, the POD mode analysis also shows the presence of another interface between p3 and p4. The Reynolds number of this interface increases as the turbulence intensity decreases, as shown in Table III. The decreasing rate of interface p3/p4 is steeper than that of interface p1/p2.

There are other methods of using POD to estimate the critical point.[19] Figure 11 represents first ten eigenvalues ($\lambda^{(i)}$) normalized to the total energy of the eigenvalue ($\Sigma\lambda^{(i)}$) as a function of the Reynolds number. High peak is clearly seen for mode 1 (blue line), near the critical Reynolds number characterized by the reattachment length (Cr_1).
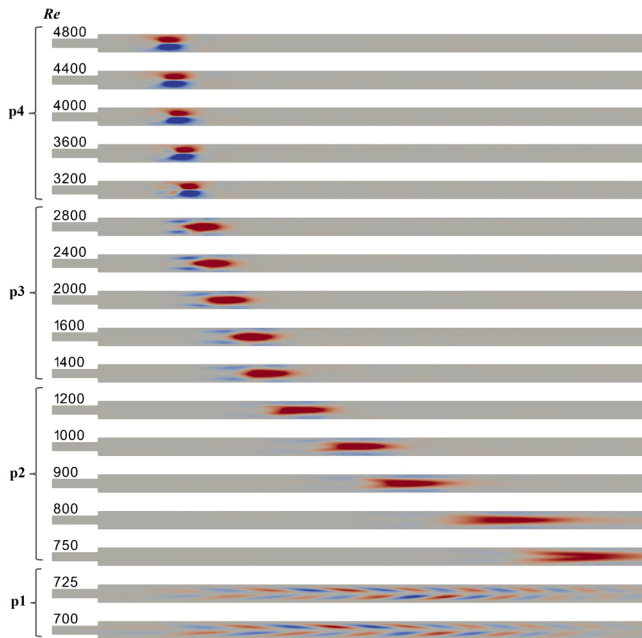
FIG. 10. Contour graph of the first mode and its classification with varying Re and $TI = 2\%$.

FIG. 11. Variation of normalized eigenvalue $\lambda^{(i)}$ for varying Re with constant TI: (a) $TI = 0.2\%$, (b) $TI = 2\%$, and (c) $TI = 10\%$.

D. Overall correlation for reattachment length

In Fig. 12, curve fits for normalized reattachment length calculated using the LES approach as a function of the Reynolds number for the laminar, transitional, and turbulent regions are presented. An overall expression for the reattachment length of axisymmetric expansion flow is suggested in this section. Li and Djilali[39] presented an analysis for general flow including separation bubble (or flow recirculation) by using scaling analysis of the Navier–Stokes equation. The solution has three different parts: linear expression; a curve with an inverse relation to Re; and a constant. Papadopoulos' scaling analysis[40] includes the effect of the inlet flow condition and has two equations describing laminar [S_L, Eq. (15)] and turbulent [S_T, Eq. (16)] flow regions, respectively. The laminar region is the one in which the reattachment length linearly increases with the Reynolds number [Eq. (15)]. On the contrary, in the turbulent region, the reattachment
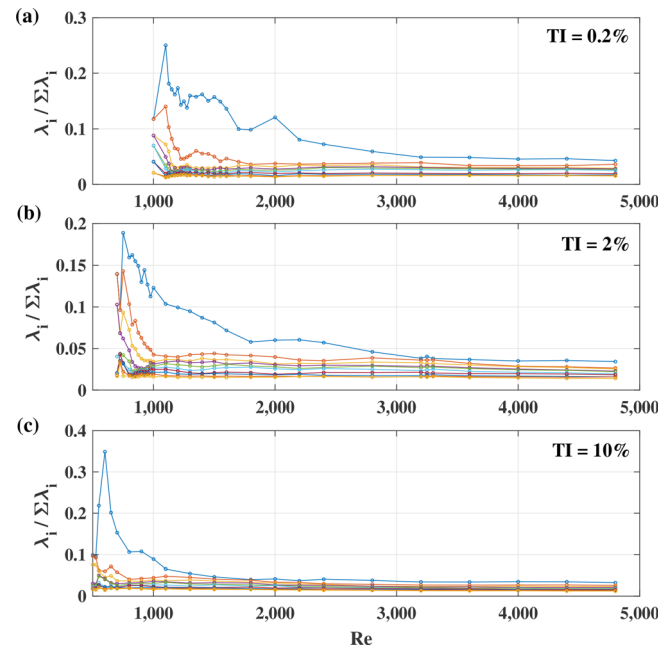
length is inversely proportional to the Reynolds number [Eq. (16)]. If the Reynolds number goes to infinity, only the constant coefficient D remains in [Eq. (16)], consistent with the current calculations that the reattachment length is independent of the Reynolds number,

$$S_L = Lr/h = A(Re - B), \tag{15}$$
$$S_T = Lr/h = C/Re + D. \tag{16}$$

Avila and Hof[41] showed that laminar-turbulence intermittency is an intrinsic feature of shear flow. The flow switched intermittently between the turbulent and laminar flow regimes. Papadopoulos[40] introduced the intermittency factor λ, and a solution for the transition region can be expressed as proportional summation between solutions for laminar and turbulent regions as written as follows:

$$S = (1 - \lambda)S_L + \lambda S_T, \tag{17}$$

TABLE III. Critical Reynolds number.

| TI (%)	Re_c Lr/h [Eq. (13)]	Re_c $\lambda^{(i)}$ (Fig. 11)	Interface by first mode's pattern (Fig. 10 and supplementary material Figs. S1–S7)		
			p1/p2	p2/p3	p3/p4
0.2	1 198.90	1075	$1050 < \mathrm{Re} < 1075$	$1800 < \mathrm{Re} < 2000$	$5400 < \mathrm{Re} < 6000$
0.5	1 059.89	950	$900 < \mathrm{Re} < 925$	$1400 < \mathrm{Re} < 1500$	$4400 < \mathrm{Re} < 4800$
1	954.73	850	$800 < \mathrm{Re} < 850$	$1250 < \mathrm{Re} < 1400$	$3200 < \mathrm{Re} < 3600$
2	849.58	750	$700 < \mathrm{Re} < 725$	$1200 < \mathrm{Re} < 1300$	$2800 < \mathrm{Re} < 3200$
5	710.56	600	$600 < \mathrm{Re} < 625$	$1000 < \mathrm{Re} < 1100$	$2000 < \mathrm{Re} < 2200$
10	605.41	525	$575 < \mathrm{Re} < 600$	$700 < \mathrm{Re} < 800$	$1300 < \mathrm{Re} < 1400$
20	500.25	$\cdots$	$500 < \mathrm{Re} < 525$	Not distinct	$1000 < \mathrm{Re} < 1100$
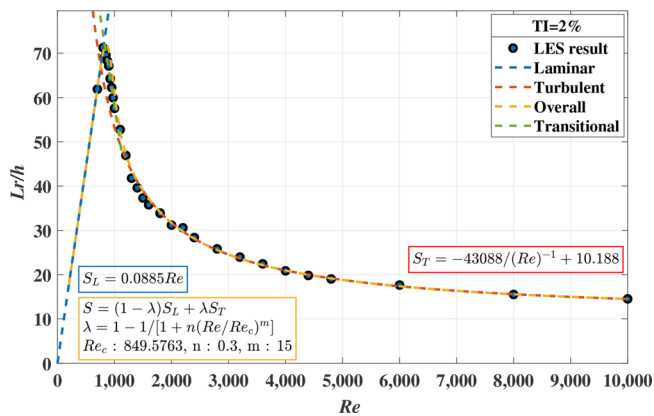
FIG. 12. Curve fitting for laminar, transition, and turbulent regions.

where $\lambda = 1 - 1/[1 + n(Re/Re_c)^m]$ is the intermittency factor with parameters n and m and Re_c is the critical Reynolds number for the laminar region.

In this paper, coefficients in Eqs. (15)–(17) are estimated by using a parametric study. The value of coefficients is estimated for each constant turbulence intensity, and their relationships are established. The LES results are divided into three different regions based on the critical point expressions suggested in this paper [Eqs. (13) and (14)] and used for obtaining expressions for coefficients. A curve fitting tool in MATLAB R2020a was employed. Figure 12 shows how coefficients are divided into three different regions and how they are estimated. Coefficients A and B in Eq. (15) do not depend on the turbulence intensity as shown in Fig. 5 and are estimated as 0.088 5 and 0, respectively. Coefficients C and D in Eq. (16) can be expressed as the function of turbulence intensity as shown in Eqs. (18c) and (18d) and Fig. 13. The coefficients for the expression yield

$$A = 0.088\,5, \tag{18a}$$

$$B = 0, \tag{18b}$$

$$C = 72\,527.81\,(\mathbf{TI}[\%])^{-0.22} - 18\,430.95, \tag{18c}$$

$$D = 10.28/(1 + (\mathbf{TI}[\%]/15.00)^{1.95}). \tag{18d}$$

Once the coefficient expression for the laminar and turbulent flow regions and the critical Reynolds number [Eq. (13)] are
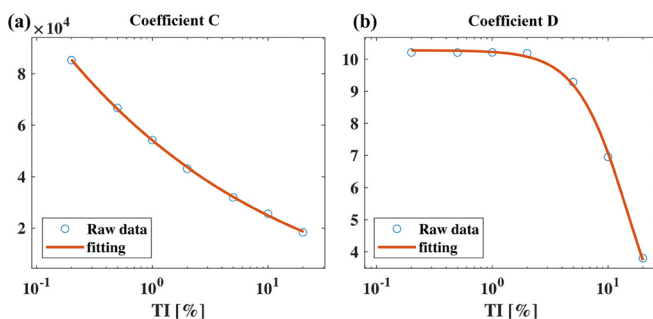

FIG. 13. Curve fits for (a) coefficient C [Eq. (18c)] and coefficient D [Eq. (18d)].

determined, coefficients n and m in the intermittency factor λ are estimated. Coefficients n and m are determined to be 0.3 and 15, respectively, to minimize the total error, which are defined as the summation of the relative error between the entire LES results and the curve fitted expression Eq. (17). The correlation has the maximum error of 10% compared with the LES results for TI $\leq$ 10% and that of 17.3% for TI = 20% near the laminar critical point. For most cases, the error is under 5%, which is an acceptable error band for the correlation. A dashed line in Fig. 5 represents the overall correlation of Eq. (17) as a function of the Reynolds number, which fits well with the LES results depicted as same-colored markers on the figure. Each color represents a different turbulence intensity.

IV. CONCLUSIONS

Large Eddy simulations were performed for flows through an axisymmetric sudden expansion to investigate the effects of the inlet condition such as the Reynolds number and turbulence intensity. The reattachment lengths calculated in the present study are in good agreement with the experimental results[15,16] and numerical simulations in the literature[28] with the proper introduction of turbulence intensity values in the range of 0.2%–20% as seen in Fig. 5. It can be concluded that the turbulence intensity (TI), a commonly used parameter to quantify flow disturbance, captures the impact of the effect of flow disturbance not only on the reattachment length but also on critical threshold values for dividing laminar/transition and transition/turbulent regions of axisymmetric sudden expansion flows.

Three critical points are observed in a flow through an axisymmetric sudden expansion and investigated in this study. The laminar region can be defined as the region that the reattachment length is independent to turbulent disturbance at the inlet for a given Reynolds number, whereas the reattachment length decreases as the turbulence intensity decreases in the transition region. This threshold value is denoted Cr_1, and the correlation is established as Eq. (13). This critical point is also clearly seen in the region between the patterns p1 and p2 calculated from mode 1 of the POD analysis (Fig. 10) and corresponds to the peak eigenvalue of mode 1 (Fig. 11). The second critical point Cr_2 is the crossover point of two curve fitted lines with different slopes observed on TI vs Lr graph (Fig. 6). The correlation expression achieved in this study is Eq. (14). The key characteristic of this critical point is that reattachment lengths obtained above this critical Reynolds number can be represented by $Lr \sim 1/Re$ regardless of turbulence intensity at the inlet. We determined that flow conditions above Cr_2 are in the turbulent region. This critical region is also seen in the POD analysis. The critical point between the patterns p2 and p3 of mode 1 might be a candidate for the Cr_2 but requires processing of inordinate amounts of data. POD mode analysis also clearly presents another interface between p3 and p4. However, further study is necessary to understand its physical meaning.

Finally, universal correlation for the reattachment length is established [Eq. (17)]. One of the reasons why there is no consensus on the critical value of flow disturbance is that many of the studies reported in the literature try to develop one curve fit equation for both transitional and turbulent regions. However, in this study, not only correlations for reattachment length for laminar, transition, and turbulent regions are presented, but also an universal curve fit is presented [Eq. (17)]. Equation (15) and its coefficients A and B [Eqs. (18a) and (18b)] are employed for the region below the Cr_1, whereas Eq. (16) and its

coefficients C and D are employed for the region [Eqs. (18c) and (18d)] above Cr_2. The transition region between Cr_1 and Cr_2 can be expressed as a summation of solutions for laminar and turbulent regions with an intermittency factor λ [Eq. (17)]. The intermittency factor λ can be calculated with parameter Cr_1 [Eq. (13)], $n = 0.3$ and $m = 15$. Since the intermittency factor goes to zero in the laminar region while going to unity in the turbulent region, this expression can be used for both laminar and turbulent regions. The correlation expression for the reattachment length normalized to the step height can be expressed as a function of the Reynolds number and turbulence intensity for $500 \leq Re \leq 15\,000$ and $0.2\% \leq TI \leq 10\%$ within 10% error. Error might increase up to 32% at $TI = 20\%$.

SUPPLEMENTARY MATERIAL

See the supplementary material for the entire contour of eigen-mode achieved from the POD analysis used in Table III.

ACKNOWLEDGMENTS

AUTHOR DECLARATIONS
Conflict of Interest

The authors have no conflicts to disclose.

Author Contributions

Byung-Hee Choi: Conceptualization (lead); data curation (lead); formal analysis (lead); investigation (lead); methodology (lead); resources (lead); software (lead); validation (lead); visualization (lead); writing – original draft (lead). **N. K. Anand:** Funding acquisition (lead); project administration (equal); supervision (equal); writing – review & editing (equal). **Yassin A. Hassan:** Supervision (equal); writing – review & editing (equal). **Piyush Sabharwall:** Project administration (equal).

DATA AVAILABILITY

The data that support the findings of this study are available within the article and its supplementary material.

REFERENCES

[1]T. Balakhrisna, S. Ghosh, G. Das, and P. Das, "Oil–water flows through sudden contraction and expansion in a horizontal pipe—Phase distribution and pressure drop," Int. J. Multiphase Flow **36**, 13–24 (2010).

[2]K. Schirrmann, G. Cáceres-Aravena, and A. Juel, "Self-assembly of coated microdroplets at the sudden expansion of a microchannel," Microfluid. Nanofluid. **25**, 29 (2021).

[3]J. W. Baughn, M. A. Hoffman, R. K. Takahashi, and D. Lee, "Heat transfer downstream of an abrupt expansion in the transition Reynolds number regime," J. Heat Transfer **109**, 37–42 (1987).

[4]H. Gach and I. Lowe, "Measuring flow reattachment lengths downstream of a stenosis using MRI," J. Magn. Reson. Imaging **12**, 939–948 (2000).

[5]B.-H. Choi, D. Orea, R. Chavez, N. K. Anand, and P. Sabharwall, "Numerical study of multi-component flow and mixing in a scaled fission product venting system," Nucl. Eng. Des. **391**, 111714 (2022).

[6]M. C. Chaturvedi, "Flow characteristics of axisymmetric expansions," J. Hydraul. Div. **89**, 61–92 (1963).

[7]B. T. Yang and M. H. Yu, "The flow field in a suddenly enlarged combustion chamber," AIAA J. **21**, 92–97 (1983).

[8]L. Khezzar, J. H. Whitelaw, and M. Yianneskis, "Round sudden-expansion flows," Proc. Inst. Mech. Eng., Part C **200**, 447–455 (1986).

[9]R. M. C. So, "Inlet centerline turbulence effects on reattachment length in axisymmetric sudden-expansion flows," Exp. Fluids **5**, 424–426 (1987).

[10]R. M. C. So and S. A. Ahmed, "Rotation effects on axisymmetric sudden-expansion flows," J. Propul. Power **4**, 270–276 (1988).

[11]R. P. Durrett, W. H. Stevenson, and H. D. Thompson, "Radial and axial turbulent flow measurements with an LDV in an axisymmetric sudden expansion air flow," J. Fluids Eng. **110**, 367–372 (1988).

[12]E. Lukács and J. Vad, "Flow topology and loss analysis of a square-to-square sudden expansion relevant to HVAC systems: A case study," J. Build. Eng. **41**, 102802 (2021).

[13]A. Iribarne, F. Frantisak, R. L. Hummel, and J. W. Smith, "An experimental study of instabilities and other flow properties of a laminar pipe jet," AIChE J. **18**, 689–698 (1972).

[14]L. H. Back and E. J. Roschke, "Shear-layer flow regimes and wave instabilities and reattachment lengths downstream of an abrupt circular channel expansion," J. Appl. Mech. **39**, 677–681 (1972).

[15]D. J. Latornell and A. Pollard, "Some observations on the evolution of shear layer instabilities in laminar flow through axisymmetric sudden expansions," Phys. Fluids **29**, 2828–2835 (1986).

[16]B. Pak, Y. I. Cho, and S. U. Choi, "Separation and reattachment of non-Newtonian fluid flows in a sudden expansion pipe," J. Non-Newtonian Fluid Mech. **37**, 175–199 (1990).

[17]K. R. Sreenivasan and P. J. Strykowski, "An instability associated with a sudden expansion in a pipe flow," Phys. Fluids **26**, 2766–2768 (1983).

[18]T. Mullin, J. R. T. Seddon, M. D. Mantle, and A. J. Sederman, "Bifurcation phenomena in the flow through a sudden expansion in a circular pipe," Phys. Fluids **21**, 014110 (2009).

[19]N. Furuichi, Y. Takeda, and M. Kumada, "Spatial structure of the flow through an axisymmetric sudden expansion," Exp. Fluids **34**, 643–650 (2003).

[20]K. Selvam, J. Peixinho, and A. P. Willis, "Localised turbulence in a circular pipe flow with gradual expansion," J. Fluid Mech. **771**, R2 (2015).

[21]E. Sanmiguel-Rojas, C. del Pino, and C. Gutiérrez-Montes, "Global mode analysis of a pipe flow through a 1:2 axisymmetric sudden expansion," Phys. Fluids **22**, 071702 (2010).

[22]D. Fletcher, S. Maskell, and M. Patrick, "Heat and mass transfer computations for laminar flow in an axisymmetric sudden expansion," Comput. Fluids **13**, 207–221 (1985).

[23]N. Moallemi and J. Brinkerhoff, "Instability and localized turbulence associated with flow through an axisymmetric sudden expansion," Int. J. Heat Fluid Flow **72**, 161–173 (2018).

[24]E. Sanmiguel-Rojas and T. Mullin, "Finite-amplitude solutions in the flow through a sudden expansion in a circular," J. Fluid Mech. **691**, 201–213 (2012).

[25]B. Lebon, M. Q. Nguyen, J. Peixinho, M. S. Shadloo, and A. Hadjadj, "A new mechanism for periodic bursting of the recirculation region in the flow through a sudden expansion in a circular pipe," Phys. Fluids **30**, 031701 (2018).

[26]M. Q. Ngyuen, M. S. Shadloo, A. Hadjadj, B. Lebon, and J. Peixinho, "Perturbation threshold and hysteresis associated with the transition to turbulence in sudden expansion pipe flow," Int. J. Heat Fluid Flow **76**, 187–196 (2019).

[27]D. V. Shenoy, M. S. Shadloo, J. Peixinho, and A. Hadjadj, "Direct numerical simulations of laminar and transitional flows in diverging pipes," Int. J. Numer. Methods Heat Fluid Flow **30**, 75–92 (2019).

[28]R. D. Luciano, X. Chen, and D. Bergstrom, "Discretization and perturbations in the simulation of localized turbulence in a pipe with a sudden expansion," J. Fluid Mech. **935**, A20 (2022).

[29]B. Lebon, J. Peixinho, S. Ishizaka, and Y. Tasaka, "Subcritical transition to turbulence in a sudden circular pipe expansion," J. Fluid Mech. **849**, 340–354 (2018).

[30]F. Nicoud and F. Ducros, "Subgrid-scale stress modelling based on the square of the velocity gradient tensor," Flow, Turbul. Combust. **30**, 183–200 (1999).

[31]K. Selvam, J. Peixinho, and A. P. Willis, "Flow in a circular expansion pipe flow: Effect of a vortex perturbation on localised turbulence," Fluid Dyn. Res. **48**, 061418 (2016).

[32]C. Howard, S. Gupta, A. Abbas, T. A. Langrish, and D. F. Fletcher, "Proper orthogonal decomposition (POD) analysis of CFD data for flow in an axisymmetric sudden expansion," Chem. Eng. Res. Des. **123**, 333–346 (2017).

[33]P. J. Roache, "Perspective: A method for uniform reporting of grid refinement studies," J. Fluids Eng. **116**, 405–413 (1994).

[34]H. Li, N. K. Anand, Y. A. Hassan, and T. Nguyen, "Large eddy simulation of the turbulence flows of twin parallel jets," Int. J. Heat Mass Transfer **129**, 1263–1273 (2019).

[35]K. Taira, S. L. Brunton, S. T. Dawson, C. W. Rowley, T. Colonius, B. J. McKeon, O. T. Schmidt, S. Gordeyev, V. Theofilis, and L. S. Ukeiley, "Modal analysis of fluid flows: An overview," AIAA J. **55**, 4013 (2017).

[36]J. Lumley, "Coherent structures in turbulence," in *Transition and Turbulence* (Academic Press, 1981), pp. 215–242.

[37]L. Sirovich and M. Kirby, "Low-dimensional procedure for the characterization of human faces," J. Opt. Soc. Am. A **4**, 519–524 (1987).

[38]D. Drikakis, "Bifurcation phenomena in incompressible sudden expansion flows," Phys. Fluids **9**, 76–87 (1997).

[39]X. Li and N. Djilali, "On the scaling of separation bubbles," JSME Int. J., Ser. **38**, 541–548 (1995).

[40]G. Papadopoulos, "A functional relationship for modeling laminar to turbulent flow transitions," J. Fluids Eng. **139**, 091202 (2017).

[41]M. Avila and B. Hof, "Nature of laminar-turbulence intermittency in shear flows," Phys. Rev. E **87**, 063012 (2013).